arXiv:astro-ph/0701643v1 23 Jan 2007

The g-mode Excitation in the Proto Neutron Star by the Standing Accretion Shock Instability

Shijun Yoshida

Science and Engineering, Waseda University,
3-4-1 Okubo, Shinjuku, Tokyo 169-8555, Japan

`yoshida@heap.phys.waseda.ac.jp`

Naofumi Ohnishi

Department of Aerospace Engineering, Tohoku University,
6-6-01 Aramaki-Aza-Aoba, Aoba-ku, Sendai 980-8579, Japan

`ohnishi@cfd.mech.tohoku.ac.jp`

and

Shoichi Yamada[1]

Science and Engineering, Waseda University,
3-4-1 Okubo, Shinjuku, Tokyo 169-8555, Japan

`shoichi@waseda.jp`

ABSTRACT

The so-called "acoustic revival mechanism" of core-collapse supernova proposed recently by the Arizona group is an interesting new possibility. Aiming to understand the elementary processes involved in the mechanism, we have calculated the eigen frequencies and eigen functions for the g-mode oscillations of a non-rotating proto neutron star. The g-modes have relatively small eigen frequencies. Since there is a convective region inside the proto neutron star, the eigen functions are confined either to the exterior or interior of this evanescent region although some fraction of eigen functions penetrates it because of their long wave lengths. The possible excitation of these modes by the standing accretion shock instability, or SASI, is discussed based on these eigen functions.

---

[1] Advanced Research Institute for Science and Engineering, Waseda University, 3-4-1 Okubo, Shinjuku, Tokyo 169-8555, Japan

We have formulated the forced oscillations of g-modes by the external pressure perturbations exerted on the proto neutron star surface. The driving pressure fluctuations have been adopted from our previous computations of the axisymmetric SASI in the non-linear regime. We have paid particular attention to low ℓ modes, since these are the modes that are dominant in SASI and that the Arizona group claimed played an important role in their acoustic revival scenario. Here ℓ is the index of the spherical harmonic functions, Y_ℓ^m. Although the frequency spectrum of the non-linear SASI is broadened substantially by non-linear couplings, the typical frequency is still much smaller than those of g-modes, the fact leading to a severe impedance mismatch. As a result, the excitations of various g-modes are rather inefficient and the energy of the saturated g-modes is $\sim 10^{50}$erg or smaller, with the g_2 mode being the largest in our model. Here the g_2 mode has two radial nodes and is confined to the interior of the convection region. The energy transfer rate from the g-modes to out-going sound waves is estimated from the growth of the g-modes and found to be $\sim 10^{51}$erg/s in the model studied in this paper.

Subject headings: supernovae: collapse — neutrinos — hydrodynamics — instability

1. Introduction

The mechanism of core-collapse supernovae has been an open question for decades. In the past 15 years, a lot of detailed numerical simulations have been done by many authors, paying attention to various aspects of the dynamics (see, for example, Kotake et al. (2006) for the latest review of the subject). Spherically symmetric models have incorporated full general relativity and solved the radiation-hydrodynamical equations with realistic equations of state and neutrino physics (Rampp & Janka 2000; Thompson et al. 2003; Liebendörfer et al. 2005; Sumiyoshi et al. 2005). These computations demonstrated consistently that the stalled shock wave is highly unlikely to be revived by neutrino heatings in the spherically symmetric dynamics.

Multi-dimensional simulations have been also making a remarkable progress over the times (see Kotake et al. (2006) and references therein). Local non-spherical motions of convection-type are common in the envelope as inferred from the spectra and light curves (Nomoto et al. 2006), and are believed to occur also in the core. The global asymmetry as observed in the ejecta of SN1987A is also supposed to be common to the core-collapse supernovae (Wang et al. 2002). Motivated by these observations, the implications of the asymmetry for the explosion mechanism have been investigated intensively and extensively (see again Kotake et al. (2006) and references therein).

Recently, the instability of the standing accretion shock wave was discovered by Blondin et al. (2003) in the context of core-collapse supernova and its nature has been studied both analytically (Foglizzo et al. 2006; Yamasaki & Yamada 2006) and numerically (Blondin & Mezzacappa 2006a; Ohnishi et al. 2006a; Blondin & Mezzacappa 2006b). The ramifications to the global asymmetry of the ejecta as mentioned above and the high kick velocities of young pulsars (Lyne & Lorimer 1994) were discussed by Scheck et al. (2004) in more realistic simulations. Since it has been demonstrated (Herant et al. 1994; Janka & Müller 1996; Yamasaki & Yamada 2006) over the years that these instabilities tend to facilitate the shock revival by neutrino heatings, attempts have been done with little success (Buras et al. 2006) so far to show by realistic multi-dimensional simulations that an explosion is indeed induced.

This situation may change. Very recently, Burrows et al. (2006a,b,c) have proposed a new possibility to induce explosions. They have done long-term simulations of axisymmetric 2D radiation-hydrodynamics. Although some microphysics are incomplete and the formulation is essentially non-relativistic, their models with no equatorial symmetry and artificial inner boundary condition being imposed have obtained a shock revival after a rather long delay ($\gtrsim$ 500ms after bounce) not by the neutrino heatings but by what they call the "acoustic" mechanism. They have claimed that the turbulence of accreted matter induces mainly g-mode oscillations in the proto neutron star, which in turn emit acoustic waves that are dissipated as they propagate outward to become shock waves.

This is a quite new idea that has eluded the discovery by multi-dimensional numerical studies for many years, the reasons for which are, the authors think, that previous computations were not long enough and/or put too restrictive conditions such as the artificial inner boundary that has been frequently employed to reduce the CFL constraint on numerical time steps. Burrows et al. (2006a,b,c) have insisted that the merit of this mechanism is the self-regulation in such a way that the g-mode excitations and subsequent emissions of acoustic waves are maintained until the shock revival occurs. This is an interesting possibility and certainly worth further exploration.

There are indeed a lot of things remaining to be clarified. First of all, the mechanism seems to be rather inefficient in transferring the energy. Inferred from the published results, the explosion energy appears to be substantially smaller than the canonical value. Since the mechanism constitutes of multiple steps, the efficiency of the couplings between different steps should be understood. For that purpose, we think that the linear analysis utilizing an idealized model that mimics the realistic situation is more suitable than large scale simulations. In this paper, we calculate the eigen frequencies and eigen functions of the

g-modes in a non-rotating proto neutron star. Assuming that the standing accretion shock instability (SASI) is responsible for the excitation of the g-modes in the acoustic mechanism, we estimate the efficiency, formulating and solving the equations for forced oscillations of the g-modes. In so doing, we use the pressure fluctuations in SASI that we obtained in the previous numerical studies (Ohnishi et al. 2006a). The emissions of acoustic waves by these excited g-modes are currently being investigated numerically and will be published elsewhere (Ohnishi et al. 2006b).

The organization of the paper is as follows. In section 2, we describe the models of proto neutron star and formulate the basic equations for the normal modes and their forced oscillations. The SASI that we use as an external force to drive the oscillations of g-modes is also presented there. We give the numerical results in section 3. We conclude the paper in section 4 with some discussions.

2. Models & Formulations

We will investigate the g-mode excitations in the proto neutron star, one of the key steps in the acoustic mechanism, under the following assumptions: (i) A non-rotating proto neutron star is approximately in hydrostatic equilibrium. (ii) SASI in the accreting matter is responsible for the excitations of g-modes. (iii) The oscillation amplitudes in the proto neutron star are small compared with the radius. As shown in the numerical simulations done by Burrows et al. (2006a,b,c), these assumptions are reasonable after the stagnation of a prompt shock wave until the excited g-modes grow sufficiently and their non-linear effects on the dynamics become significant. Then the dynamics of the proto neutron star can be treated by the linear perturbation theory formulated below.

The linear perturbation of stars can be described in terms of the Lagrangian displacement $\boldsymbol{\xi}(t, \mathbf{r})$, which obeys the equation of motion given as

$$\frac{\partial^2 \boldsymbol{\xi}}{\partial t^2} + \mathbf{C} \cdot \boldsymbol{\xi} = \mathbf{F}\,, \tag{1}$$

where $\mathbf{C}$ and $\mathbf{F}$ are, respectively, the self-adjoint operator and the external force driving the perturbations (see, e.g., Friedman & Schutz 1978; Unno et al. 1989). Here, we have assumed the unperturbed star to be static and spherically symmetric. Assuming the Lagrangian displacement to be

$$\boldsymbol{\xi}(t, \mathbf{r}) = \boldsymbol{\xi}_\alpha(\mathbf{r}) e^{i\omega_\alpha t}\,, \tag{2}$$

where $\boldsymbol{\xi}_\alpha$ and ω_α are the eigen function and eigen frequency, respectively, we can obtain the normal mode solutions, for which the eigen function and eigen frequency satisfy the following equation,

$$-\,\omega_\alpha^2\,\boldsymbol{\xi}_\alpha(\mathbf{r})+\mathbf{C}\cdot\boldsymbol{\xi}_\alpha(\mathbf{r})=0\,. \tag{3}$$

Here, $\{\alpha\}$ denotes the mode index, which includes for spherical stars the angular eigen values ℓ and m (see below) and the radial mode number n. We impose for the normal mode solutions the regularity condition at the stellar center and $\delta p=0$ at the stellar surface, where δp stands for the Lagrangian change of the pressure p.

When the unperturbed star is static and spherically symmetric, the orthogonality of the eigen functions allows us to adopt the normalization

$$\int d^3\mathbf{r}\,\rho(r)\,\boldsymbol{\xi}^*_{\alpha'}(\mathbf{r})\cdot\boldsymbol{\xi}_\alpha(\mathbf{r})=MR^2\delta_{\alpha'\alpha}\,, \tag{4}$$

where ρ, M and R denote the density, mass and radius of the unperturbed star, respectively (see, e.g., Unno et al. 1989). Any Lagrangian displacement $\boldsymbol{\xi}$ that satisfies the same boundary conditions as those for the normal modes is then expressed as the linear superposition of the normal modes:

$$\boldsymbol{\xi}(t,\mathbf{r})=\sum_\alpha A_\alpha(t)\boldsymbol{\xi}_\alpha(\mathbf{r})\,. \tag{5}$$

Substituting Eq. (5) into Eq. (1) and using Eqs. (3) and (4), we obtain the dynamical equation for the expansion coefficient $A_\alpha(t)$ as

$$\frac{d^2A_\alpha(t)}{dt^2}+\omega_\alpha^2A_\alpha(t)=\frac{1}{MR^2}\int d^3\mathbf{r}\,\rho(r)\,\boldsymbol{\xi}^*_\alpha(\mathbf{r})\cdot\mathbf{F}(t,\mathbf{r})\,. \tag{6}$$

2.1. Normal mode oscillations

In this paper, we study adiabatic oscillations of a non-rotating spherical proto neutron star and employ the Cowling approximation, neglecting perturbations of the gravitational potential (see, e.g., Unno et al. 1989). For spherical stars, the separation of the angular variables in the perturbation equations can be achieved by the use of the spherical harmonics in the spherical polar coordinates $(r,\,\theta,\,\phi)$. The Lagrangian displacement vector $\boldsymbol{\xi}$ is expressed in terms of the vector spherical harmonics as

$$(\xi_r,\,\xi_\theta,\,\xi_\phi)=\left(ry_1(r),\,rh(r)\frac{\partial}{\partial\theta},\,rh(r)\frac{1}{\sin\theta}\frac{\partial}{\partial\phi}\right)Y_\ell^m(\theta,\phi)\,e^{i\omega t}\,, \tag{7}$$

and the Eulerian perturbation of pressure p' is given by

$$p'=\rho\,g\,ry_2(r)\,Y_\ell^m(\theta,\phi)\,e^{i\omega t}\,, \tag{8}$$

where g denotes the local gravitational acceleration. Eq. (3) is then reduced to

$$z\frac{dy_1}{dz} = (V_g - 3)\, y_1 + \left(\frac{l(l+1)}{c_1\bar{\omega}^2} - V_g\right) y_2\,, \tag{9}$$

$$z\frac{dy_2}{dz} = (c_1\bar{\omega}^2 + rA)\, y_1 + (-rA - U + 1)\, y_2\,, \tag{10}$$

where

$$\begin{aligned}
z &= r/p\,, && (11)\\
V_g &= \frac{V}{\Gamma} = -\frac{1}{\Gamma}\frac{d\ln p}{d\ln r}\,, && (12)\\
U &= \frac{d\ln M_r}{d\ln r}\,, && (13)\\
c_1 &= (r/R)^3/(M_r/M)\,, && (14)\\
\bar{\omega}^2 &= \omega^2 R^3/(GM)\,, && (15)\\
rA &= \frac{d\ln\rho}{d\ln r} - \frac{1}{\Gamma}\frac{d\ln p}{d\ln r}\,. && (16)
\end{aligned}$$

Here, Γ and M_r stand for the adiabatic exponent and the stellar mass contained inside the radius r, respectively. The inner and outer boundary conditions are explicitly given by

$$c_1\bar{\omega}^2 y_1 - l y_2 = 0 \quad \text{as } r \to 0\,, \tag{17}$$

$$y_1 - y_2 = 0 \quad \text{as } r \to R\,. \tag{18}$$

The total mode energy E is defined as

$$E = \frac{1}{2}\int d^3\mathbf{r}\,\rho(r)\left(\left|\frac{\partial\boldsymbol{\xi}}{\partial t}\right|^2 + \left|\frac{p'}{\rho c_s}\right|^2 + \left(\frac{g}{N}\right)^2\left|\frac{p'}{\Gamma p} - \frac{\rho'}{\rho}\right|^2\right)\,, \tag{19}$$

where ρ' is the Eulerian perturbation of density, and c_s and N mean the sound velocity and the Brunt-Väisälä frequency defined, respectively, as

$$c_s^2 = \Gamma p/\rho\,, \quad N^2 = -gA\,. \tag{20}$$

In order to obtain eigen frequencies and eigen functions, Eqs. (9) and (10) are solved numerically as an eigen value problem for $\bar{\omega}$, together with the boundary conditions (17) and (18). A Henyey-type relaxation method is employed (see, e.g., Unno et al. 1989).

Introducing new variables $\tilde{\xi}$ and $\tilde{\eta}$ defined as

$$\tilde{\xi} = r^3 y_1 \exp\left(-\int_0^r \frac{g}{c_s^2}dr\right)\,, \tag{21}$$

$$\tilde{\eta} = gry_2 \exp\left(-\int_0^r \frac{N^2}{g} dr\right) , \tag{22}$$

we can rewrite the set of the pulsation equations (9) and (10) in a canonical form given by

$$\frac{d\tilde{\xi}}{dr} = H(r)\frac{r^2}{c_s^2}\left(\frac{L_\ell^2}{\omega^2} - 1\right)\tilde{\eta} , \tag{23}$$

$$\frac{d\tilde{\eta}}{dr} = \frac{1}{r^2 H(r)}\left(\omega^2 - N^2\right)\tilde{\xi} , \tag{24}$$

where L_ℓ is the Lamb frequency defined as

$$L_\ell = c_s \frac{\sqrt{\ell(\ell+1)}}{r} . \tag{25}$$

Here, the function $H(r)$ is positive definite and is defined by

$$H(r) = \exp\left[\int_0^r \left(\frac{N^2}{g} - \frac{g}{c_s^2}\right) dr\right] . \tag{26}$$

The canonical pulsation equations (23) and (24) are more appropriate to gain the insight into the qualitative properties of nonradial oscillations. Ignoring the spatial variations of all the coefficients in Eqs. (23) and (24) and employing a WKB-type local approximation, we obtain the eigen functions in the form,

$$\tilde{\xi}(r),\ \tilde{\eta}(r) \ \propto\ \exp(ik_r r) , \tag{27}$$

where k_r means a radial wave number of the perturbations. Then the following dispersion relation is obtained:

$$k_r^2 = \frac{1}{\omega^2 c_s^2}(\omega^2 - L_\ell^2)(\omega^2 - N^2) , \tag{28}$$

which implies that if $(\omega^2 - L_\ell^2)(\omega^2 - N^2) > 0$, the wave number k_r is real and the corresponding wave can propagate in the radial direction, whereas the wave number k_r becomes purely imaginary and the amplitude of the perturbation grows or damps exponentially with r when $(\omega^2 - L_\ell^2)(\omega^2 - N^2) < 0$.

2.2. Mode excitations

In this study, we are concerned with the excitation of oscillations in the proto neutron star by the turbulence in accreting matter. In our formulation, we take into account the latter effect as pressure perturbations at the surface of proto neutron star. Hence we set $\mathbf{F} = 0$ in Eq. (1) and adopt the time-dependent non-vanishing pressure perturbation given by

$$\delta p = f(t)\, p(r)\, Y_\ell^m(\theta,\phi) \quad \text{as } r \to R \tag{29}$$

instead of the ordinary condition $\delta p = 0$ at the proto neutron star surface. Here the function of time, $f(t)$, describes how the stellar surface is disturbed by the accreted matter and is taken from the numerical results obtained in our previous exploration of SASI (see section 2.3).

Note that the boundary condition (29) is no longer the same as that for the normal modes, $\delta p = 0$ at $r = R$. However, we can still use an expansion by the normal modes, $\boldsymbol{\xi}_\alpha$, for a part of the Lagrangian displacement by introducing a new dependent variable $\boldsymbol{\eta}$ defined as

$$\boldsymbol{\eta} = \boldsymbol{\xi} + \boldsymbol{\zeta}\,, \tag{30}$$

where

$$(\zeta_r, \zeta_\theta, \zeta_\phi) = \left(r \left(\frac{1}{\Gamma}\right)_{r=R} \frac{f(t)}{\ell+3} \left(\frac{r}{R}\right)^\ell Y_\ell^m(\theta,\phi),\, 0,\, 0 \right)\,. \tag{31}$$

Substituting $\boldsymbol{\xi} = \boldsymbol{\eta} - \boldsymbol{\zeta}$ into Eq. (1), we obtain the master equation for $\boldsymbol{\eta}$ given by

$$\frac{\partial^2 \boldsymbol{\eta}}{\partial t^2} + \mathbf{C}\cdot\boldsymbol{\eta} = \frac{\partial^2 \boldsymbol{\zeta}}{\partial t^2} + \mathbf{C}\cdot\boldsymbol{\zeta}\,. \tag{32}$$

In Eq. (31), $\boldsymbol{\zeta}$ is chosen so that $\boldsymbol{\eta}$ could satisfy the same boundary conditions as those for the normal modes:

$$\delta p_\eta \;=\; -\frac{p\Gamma}{\rho}\boldsymbol{\nabla}\cdot\boldsymbol{\eta} = 0 \quad \text{at } r = R\,, \tag{33}$$

and $\boldsymbol{\eta}$ is regular at $r = 0$. As a result, we can express $\boldsymbol{\eta}$ as a linear superposition of the eigen functions for the normal modes,

$$\boldsymbol{\eta}(t,\mathbf{r}) = \sum_\alpha A_\alpha(t)\boldsymbol{\xi}_\alpha(\mathbf{r})\,. \tag{34}$$

The expansion coefficient $A_\alpha(t)$ is again determined by the equation similar to Eq. (6),

$$\frac{d^2 A_\alpha}{d\bar{t}^2} + \bar{\omega}_\alpha^2 A_\alpha = \frac{R}{GM^2}\int d^3\mathbf{r}\,\rho(r)\,\boldsymbol{\xi}_\alpha^*(\mathbf{r})\cdot\left(\frac{\partial^2\boldsymbol{\zeta}}{\partial t^2} + \mathbf{C}\cdot\boldsymbol{\zeta}\right) = \frac{R}{GM^2}S_\alpha\,, \tag{35}$$

where $\bar{t} = t(GM/R^3)^{1/2}$. In Eq. (35), the driving-force term $(R/GM^2)S_\alpha$ is explicitly written as

$$\frac{R}{GM^2} S_\alpha = a f(\bar{t}) + b \frac{\partial^2 f(\bar{t})}{\partial \bar{t}^2}\,, \tag{36}$$

where a and b are constants determined by the background structure of the proto neutron star and the eigen functions for the normal modes and are given as

$$\begin{aligned} a &= \left(\frac{1}{\Gamma}\right)_{r=R} \int_0^1 dx\, \frac{\rho R^3}{M} x^{\ell+2} \left[\frac{Rp}{GM\rho} \left(\frac{1}{\ell+3} V_g - 1 \right) V (y_2^* - y_1^*) \right. \\ &\qquad \left. - \frac{x^2}{c_1} \left\{ \frac{1}{\ell+3} (rA - V_g) + 1 \right\} y_1^* \right]\,, \qquad (37) \\ b &= \left(\frac{1}{\Gamma}\right)_{r=R} \int_0^1 dx\, \frac{\rho R^3}{M} x^{\ell+4} \frac{y_1^*}{\ell+3}\,. \qquad (38) \end{aligned}$$

Here the normalized radius $x = r/R$ is introduced.

Once we obtain $A_\alpha(t)$, the Lagrangian displacement vector $\boldsymbol{\xi}$ is given by

$$\boldsymbol{\xi}(t, \mathbf{r}) = \sum_\alpha A_\alpha(t) \boldsymbol{\xi}_\alpha(\mathbf{r}) - \boldsymbol{\zeta}\,. \tag{39}$$

Since $\boldsymbol{\zeta}$ does not satisfy, in general, the orthogonality,

$$\int d^3\mathbf{r}\, \rho(r)\, \boldsymbol{\xi}_\alpha^*(\mathbf{r}) \cdot \boldsymbol{\zeta} = 0\,, \tag{40}$$

$\boldsymbol{\zeta}$ includes the components proportional to $\boldsymbol{\xi}_\alpha$, and the expansion coefficient $A_\alpha(t)$ is only a part of the excited oscillation mode. The true amplitude $B_\alpha(t)$ of the excited mode $\boldsymbol{\xi}_\alpha$ in $\boldsymbol{\xi}$ can be obtained by the inner product between $\boldsymbol{\xi}$ and $\boldsymbol{\xi}_\alpha$ as

$$B_\alpha(t) = \frac{1}{MR^2} \int d^3\mathbf{r}\, \rho(r)\, \boldsymbol{\xi}_\alpha^*(\mathbf{r}) \cdot \boldsymbol{\xi} = A_\alpha(t) - \frac{1}{MR^2} \int d^3\mathbf{r}\, \rho(r)\, \boldsymbol{\xi}_\alpha^*(\mathbf{r}) \cdot \boldsymbol{\zeta}\,. \tag{41}$$

Substituting Eqs. (7) and (31) into Eq. (41), we obtain

$$B_\alpha(t) = A_\alpha(t) - b f(t)\,. \tag{42}$$

It is reasonable to assume that no modes are excited in the proto neutron star initially, i.e., $B_\alpha(t) = 0$ and $dB_\alpha(t)/dt = 0$ at $t = 0$. Accordingly, we start the integration of Eq. (35) with the following initial conditions,

$$A_\alpha(t) = b f(t)\,, \quad \frac{dA_\alpha(t)}{dt} = b \frac{df(t)}{dt} \quad \text{at} \ \ t = 0\,. \tag{43}$$

2.3. SASI

As already mentioned above, we assume in this paper that oscillations in the proto neutron star are excited by the turbulence of accreting matter, which is supposed to be induced by SASI. SASI is a non-local hydrodynamical instability that occurs in the accretion flow through the standing shock wave onto the proto neutron star (Blondin et al. 2003; Scheck et al. 2004; Blondin & Mezzacappa 2006a; Ohnishi et al. 2006a; Blondin & Mezzacappa 2006b). Although the mechanism is still controversial (Blondin & Mezzacappa 2006a), SASI is probably driven by the cycle of inward advections of entropy- and vortex-perturbations and outward propagations of pressure fluctuations (Foglizzo et al. 2006; Yamasaki & Yamada 2006).

The prominent feature of SASI is the dominance of low ℓ modes both in the linear and non-linear regimes. In particular, the $\ell = 1$ mode is thought to be a promising cause for the proper motions of young pulsars. In this paper, we regard SASI as a source of pressure perturbations exerted on the surface of the proto neutron star, that is, $f(t)$ in Eq. (29).

We employ the numerical results obtained by Ohnishi et al. (2006a), in which we have done 2D axisymmetric simulations of the accretion flows through the standing shock wave onto the proto neutron star. The realistic equation of state by Shen et al. (1998) and the standard reaction rates (Bruenn 1985) for the neutrino absorptions and emissions on nucleons were employed. The mass accretion rate and the neutrino luminosity are the parameters that specify a particular steady accretion flow and were held constant during the computations. The self-gravity of the accreting matter was ignored and only the gravitational attraction by the proto neutron star was taken into account. The mass of the proto neutron star was also set to be constant ($1.4\mathrm{M}_\odot$) so that we could obtain completely steady background flows, to which velocity perturbations were added initially.

In the following, we use the results for the model with the mass accretion rate of $\dot{M} = 0.19\mathrm{M}_\odot/\mathrm{s}$ and neutrino luminosity of $L_\nu = 3 \times 10^{52}\mathrm{erg/s}$, which are typical for the post bounce core around the shock stagnation. The neutrino spectra were assumed to take a Fermi-Dirac distribution with a vanishing chemical potential and a temperature of $T_{\nu_e} = 4\mathrm{MeV}$ for the electron-type neutrino and $T_{\overline{\nu}_e} = 5\mathrm{MeV}$ for the electron-type anti-neutrino. The random velocity perturbation of less than 1% was added to the radial velocity initially. We refer the readers to Ohnishi et al. (2006a) for more detailed formulations.

We observed SASI growing exponentially in the linear phase that lasts for ∼100ms and then saturated to enter the non-linear phase. The $\ell = 1$ feature was clearly seen in the non-linear stage for this model although other modes were also generated by non-linear mode couplings. We expanded the Eulerian pressure perturbation at the inner boundary by the spherical harmonic functions. We used only the $\ell = 1$ component in this study, since this was claimed to be the most important mode (Burrows et al. 2006a,b,c).

The power spectrum of this component is shown in Fig. 1. As can be seen, the pressure perturbation is actually a series of impulsive forces that last for quite short times. It should be noted that the linear analysis of SASI for this model gives the eigen frequency of $\sim$ 30Hz for the linear $\ell = 1$ mode. The non-linear couplings broaden the spectrum both to the lower and higher frequencies. As seen later in section 3, the spectrum has most of the power in much lower frequencies than the typical g-mode frequencies of several hundreds Hz, which leads to a severe impedance mismatch in exciting g-modes.

It should be mentioned that the model studied here is not fully self-consistent. For example, what we need in Eq. (29) is the Lagrangian perturbation of pressure while what we obtained above is the Eulerian perturbation. This is simply because the former is difficult to obtain from the numerical data. Although they are different, rigorously speaking, we think that the difference will not change the outcome qualitatively, since it is the typical frequency and spectral feature of SASI that matters in this study. We should also bear in mind that the SASI spectrum employed in this study is just a single realization of essentially chaotic flows although we expect it is representative.

2.4. Proto neutron star model

Finally, the spherically symmetric, stationary proto neutron star that is adopted as the unperturbed state in this study is briefly described. The model is based essentially on the results of detailed radiation-hydrodynamical simulation of core-collapse by Sumiyoshi et al. (2005), but we have modified it in the following way.

We have developed a numerical code to compute the long-term post-bounce evolution in the quasi-steady approximation (Watanabe 2006), the details of which will be published elsewhere. In this formalism, we solve separately but consistently three different regions in the collapsing star simultaneously: (1) the proto neutron star that cools in a quasi-static way. We calculate both the equilibrium configuration and the neutrino transport in it with matter accretion taken into account. (2) the steady accretion flow from the standing shock wave down to the proto neutron star for the given neutrino luminosity obtained in the calculation (1) and matter accretion rate given by the next computation. (3) the dynamical implosion of the envelope toward the standing shock wave. The second and third regions are joined by the Rankine-Hugoniot condition at the shock wave consistently.

The code can follow the spherically symmetric quasi-static evolutions for more than 10 seconds and we have confirmed that the evolution is well reproduced for the first second, for which the result of the detailed dynamical simulations is available. In this study, we utilize the proto neutron star, which is obtained in this approximation and is in hydro-static equilibrium at ∼360ms after bounce. Physical quantities characterizing the proto neutron star model, that is, mass M, radius R, and Kepler frequency $\Omega_{\rm k}$ are given in Table 1. The profiles of density, pressure, specific entropy, and electron fraction are shown in Fig. 2 as a function of radius. It is noted that this spherically symmetric model contains a convectively unstable region around $r \sim 20$km.

Here again, the proto neutron star model is not very consistent with the model for SASI. As mentioned in the previous section, it is not our aim to construct a fully self-consistent model in this paper, where the elementary feature of the g-mode excitations is explored qualitatively from an experimental point of view. For that purpose, the slight inconsistency in the current model does not matter.

3. Results

We first consider the oscillation properties of g-modes for the proto neutron star model described in the previous section. Before giving the eigen functions, we look into the so-called propagation diagram (see, e.g., Unno et al. 1989), which is useful to see where in the star the wave with a particular frequency ω can propagate. The diagram shows the square of the Lamb frequency L_ℓ^2 and the Brunt-Väisälä frequency N^2 as a function of the normalized radius r/R. As explained in section 2, since the waves can propagate when $(\omega^2 - L_\ell^2)(\omega^2 - N^2) > 0$ is satisfied, the region where this condition holds true is called the propagation zone, and the other regions in the diagram are referred to as an evanescent zone, in which the perturbations do not oscillate but grow or damp exponentially.

Fig. 3 is the propagation diagram for the present proto neutron star model, in which we take $\ell = 1$ to calculate the Lamb frequency and the frequency is normalized according to Eq. (15). The propagation regions can be classified into two categories: one is the g-mode propagation zone indicated as hatched regions and the other is the p-mode propagation zone shown as a cross-hatched region in Fig. 3. As mentioned already, since the proto neutron star has a convective region around $r \sim 20$km, which is an evanescent zone for g-modes, there are two disconnected g-mode propagation zones, one is near the center of the star and the other near the surface. This implies that a particular g-mode is almost trapped in one of these two disconnected g-mode propagation zones. In other words, the g-modes for the current proto neutron star model are essentially divided into two classes, i.e., what we refer to as the core g-modes (g^c-modes) and the surface g-modes (g^s-modes), whose amplitudes of the eigen functions have a peak near the center and the surface of the proto neutron star, respectively.

We now discuss the properties of the normal mode oscillations obtained numerically for the current proto neutron star model. In Table 2, we summarize the key quantities for several low-order g-modes: the normalized angular eigen frequencies, $\bar{\omega}$, the corresponding frequencies in Hz, ν, the mode energies, E, and the integral quantities, a and b, defined by Eqs. (37) and (38). The last two are important in evaluating the excitations of g-modes by external perturbations in the next section. The mode energy gives us a rough measure of non-linear oscillations in the proto neutron star. Note that we employ the normalization condition for the eigen functions, Eq. (4), in evaluating the mode energy E. As expected, the mode energy is of the order of 10^{53}ergs. The typical frequency of low-order g-modes is several hundreds Hz, and we can confirm that the numbers given in Table 2 are comparable with those found by Burrows et al. (2006a). It should be also emphasized that these frequencies are much larger than the typical frequency, $\lesssim$100 Hz, of SASI in the non-linear stage. It is also recognized in Table 2 that for $\ell = 1, 2$ the lowest mode is a surface mode and core modes and surface modes appear alternately as one goes to higher overtones.

In Fig. 4, the eigen functions, y_1 and y_2 in Eqs. (7) and (8), are shown for the g-modes with $\ell = 1$ as a function of the normalized radius of the proto neutron star r/R. In the figure, the g_n-mode means the n-th radial overtone g-mode, which is characterized by n radial nodes. As mentioned just above, the g_1- and g_2-modes are a typical surface and core g-mode, respectively. In fact, the eigen functions have a non-negligible amplitude either outside or inside the convection region, which is an evanescent zone for g-modes and located at $r \sim$ 20km. This is also true for other g-modes with different ℓ or n. Upon using these eigen functions, the quantities, a and b, which appear in Eq. (36) and give the driving force for mode excitations, are obtained by integrating Eqs. (37) and (38). Although the general trend is that their absolute values decrease as the radial node number increases, there are exceptions that are critically important in determining which mode is most efficiently excited by external perturbations as explained below.

Now we move on to the excitation by accreting matter of the g-modes considered just above. As mentioned before, we assume in this study that the g-modes are excited by the pressure fluctuations around the surface of the proto neutron star, which are induced by SASI in the accretion flow. The pressure fluctuation $f(t)$ in Eq. (29) is obtained from the numerical results on SASI and is displayed in Fig. 1 as a power spectrum. It should be repeated that the major peaks of the spectrum are observed in the frequencies much lower than those of the low-order g-modes given in Table 2. In other words, the typical frequency of SASI, the driving force, is much lower than that of the low-order g-modes that should be excited in the proto neutron star. It is true that these numbers are dependent on the models of proto neutron star and SASI as well as EOS employed, but we expect that the mismatch of the frequencies is a rather generic issue.

By making use of the pressure fluctuations shown in Fig. 1 and solving Eq. (35) together with the initial condition given in Eq. (43), we calculate the time evolution of the mode amplitude, $B_\alpha(t)$, for several g-modes. Among them, the most efficiently excited g-mode is the g_2^c-mode with $\ell = 1$. This is mainly because it has the largest a as given in Table 2. In Fig. 5, we show the temporal evolution of the mode energy for the g_2^c-mode with $\ell = 1$. Since the driving forces, that is, the pressure fluctuations induced by SASI are a collection of impulsive forces, the mode energy is fluctuating on a short time scale. It is clear, however, that the mode is growing for $\sim$100ms initially and then is saturated. The maximum value of the excited mode energy is $\lesssim 10^{50}$(erg) for this mode, which is considerably smaller than the typical energy of non-linear oscillations, $\sim 10^{53}$erg, given in Table 2. In this sense, the excitation of the g-modes is inefficient, at least for the present model. This is a direct consequence of the severe mismatch in the frequencies of the driving force, SASI, and the excited g-modes. Hence it is more appropriate to refer to what we see here as the forced oscillation rather than as the excitation. It is noted, however, that the Eulerian pressure perturbations at $r \sim 50$km are found to be of the same order as those found in Burrows et al. (2006a).

The maximum values of the mode energy for other g-modes, $\lesssim 10^{49}$erg, are even smaller than that of the g_2^c-mode with $\ell = 1$ for the proto neutron star model considered here. We show in Fig. 6 the temporal evolutions of the mode energy for the g_1- and g_2-modes with $\ell = 1$. The essential feature is the same as for the g_2-mode shown in Fig. 5. These modes also grow for about 100ms initially and then get saturated with large fluctuations on a short time scale. It is emphasized again that all these excitations are non-resonant. In that case, the maximum amplitude of $\partial^2 A_\alpha(t)/\partial t^2$ can be approximated by the maximum value of $af(t)$, which, for example, becomes $\sim 10^{-2}$ for the g_2-mode and an-order-of-magnitude smaller for other modes with $\ell = 1$. From Eq. (19), we then have approximate values of the mode energies, which are consistent with the numerical results given in Figs. 5 and 6.

4. Summary and Discussions

Inspired by a series of papers on the acoustic mechanism of core-collapse supernova by Burrows et al. (2006a,b,c), we have calculated in this paper the eigen frequencies and eigen functions for several low-order g-modes in the proto neutron star, which were claimed to play an important role in the acoustic mechanism, and have studied also their excitations by

SASI in the accreting matter. We have constructed a proto neutron star model, which is supposed to represent a quasi-equilibrium configuration around a few hundred milliseconds after bounce, based on the detailed radiation-hydrodynamical simulations by Sumiyoshi et al. (2005). We have employed the temporal variation of pressure on surface of the proto neutron star, which were obtained in the study on SASI by Ohnishi et al. (2006a).

We have found that the g-modes are classified either as the surface g-mode or as the core g-mode according to the profile of the eigen function, since there is a convective zone in the proto neutron star, which is an evanescent zone for the g-modes. The eigen frequencies of the low-order g-modes are several hundred Hz, which are larger in general than the typical frequency of SASI, $\lesssim$100Hz, in the non-linear regime.

Assuming that SASI is the driving force for the g-mode excitations, we have solved numerically the equations for the time evolution of the g-mode amplitude with the pressure perturbations at the surface of the proto neutron star taken into account. We have observed that the g-mode amplitudes grow for $\sim$100ms initially and then get saturated. For the proto neutron star model considered in this paper, the g_2^c-mode, that is, the second overtone core g-mode with $\ell = 1$ is found to have the largest mode energy at saturation. Even for this mode, the mode energy, $\lesssim 10^{50}$erg, is much smaller than the typical energy, $\sim 10^{53}$erg, for non-linear oscillations, which can be estimated by imposing the natural normalization condition to the eigen functions. This apparent inefficiency of the g-mode excitations is a direct consequence of the mismatch of the frequencies of the g-modes and SASI.

It is noted, however, that what is important for the acoustic mechanism may not be the mode energy. In fact, the Burrows et al. (2006a) mentioned that the g-mode oscillations acted like a transducer that transformed the gravitational energy of accreted matter to the energy of out-going sound waves. In the present formulation, unfortunately, it is in principle impossible to obtain the energy that will be transferred to the out-going acoustic waves. However, we may be able to infer it as follows. In the growth phase that lasts for $\sim$100ms, the energy of accreting matter, or the work done by the external pressure perturbation in the present model, is transferred to the mode energy, as is apparent in Fig. 5. After saturation, on the other hand, the mode energy is almost unchanged. In this phase, then, it may be that the energy of the accreting matter is emitted just at the same rate as the accumulation rate. If this is really the case, we can estimate that the emitted energy, possibly as out-going acoustic waves, will be $\sim 10^{51}$erg/s, which may not be a bad estimate, provided, in general, the explosion is considerably delayed ($\gtrsim$500ms) in the acoustic mechanism. It is obvious, however, that more elaborate formulation of the problem, which would include the out-going waves, is required. Numerical approaches from an experimental view point will be also useful (Ohnishi et al. 2006b).

There are many other improvements remaining to be done. As repeated in the text, we have not attempted to make the model fully self-consistent in this paper, since the qualitative understanding of the g-mode excitations by SASI is the focus of the paper. However, the dependence of the results on the proto neutron star model, EOS, the progenitor model that determines the accretion rate, and so forth should be investigated in addition to making the model more self-consistent, all of which are currently under way.

This work is partially supported by the Grant-in-Aid for the 21st century COE program "Holistic Research and Education Center for Physics of Self-organizing Systems" of Waseda University and for Scientific Research (14740166, 14079202, Young Scientist (B) 17740155) of the Ministry of Education, Science, Sports and Culture of Japan.

REFERENCES

Blondin, J. M., Mezzacappa, A., & DeMarino, C. 2003, ApJ, 584, 971

Blondin, J. M., & Mezzacappa, A. 2006a, ApJ, 642, 401

Blondin, J. M., & Mezzacappa, A. 2006b, to be published in Nature, astro-ph/0611680

Buras, R., Janka, H. -Th., Rampp, M., & Kifonidis, K. 2006, A&A, 457, 281

Burrows, A., Livne, E., Dessart, L., Ott, C. D., & Murphy, J. 2006a, ApJ, 640, 878

Burrows, A., Livne, E., Dessart, L., Ott, C. D., & Murphy, J. 2006b, to be published in ApJ, astro-ph/0610175

Burrows, A., Dessart, L., Ott, C. D., & Livne, E., 2006c, To be published in the "Centennial Festschrift for Hans Bethe," Physics Reports (Elsevier: Holland), ed. G.E. Brown, E. van den Heuvel, and V. Kalogera, 2006, astro-ph/0612460

Bruenn, S. W. 1985, ApJS, 58, 771

Foglizzo, T., Scheck, L., & Janka, H. -Th. 2006, ApJ, 652, 1436

Friedman, J. L., & Schutz, B. F. 1978, ApJ, 222, 281

Herant, M., Benz, W., Hix, W. R.., Fryer, C. L., & Colgate, S. A. 1994, ApJ, 435, 339

Janka, H. -Th., & Müller, E. 1996, A&A, 306, 167

Kotake, K., Sato, K., & Takahashi, K. 2006, Rept.Prog.Phys. 69, 971-1144

Liebendörfer, M., Rampp, M., Janka, H. T., & Mezzacappa, A., 2005, ApJ, 620, 840

Lyne, A. G., & Lorimer, D. R., 1994, Nature, 369, 127

Nomoto, K., Tominaga, N., Umeda, H., Kobayashi, C., & Maeda, K. 2006, Nucl. Phys., A 777, 424

Ohnishi, N., Kotake K., & Yamada, S. 2006a, ApJ, 641, 1018

Ohnishi, N., Kotake K., & Yamada, S. 2006b, in preparation

Rampp, M., & Janka, H. -Th. 2000, ApJL, 539, L33

Scheck, L., Plewa, T., Janka, H.-Th., Kifonides, K., & Müller, E. 2004, Phys. Rev. Lett., 92, 011103

Shen, H., Toki, H., Oyamatsu, K., & Sumiyoshi, K. 1998, Nucl. Phys. A, 637, 48

Sumiyoshi, K., Yamada, S., Suzuki, S., Shen, H., Chiba, S., & Toki, H. 2005, ApJ, 629, 922

Thompson T A, Burrows A and Pinto P A 2003 ApJ, 592, 434

Unno, W., Osaki, Y., Ando, H., Saio, H., & Shibahashi, H. 1989, Nonradial Oscillations of Stars (Tokyo: Univ. Tokyo Press)

Wang, L., Wheeler, J. C., Höflich, P., Khokhlov, A., Baade, D., Branch, D., Challis, P., Filippenko, A. V., Fransson, C., Garnavich, P., Kirshner, R. P., Lundqvist, P., McRay, R., Panagia, N., Pun, C. S. J., Phillips, M. M., Sonneborn, G., & Suntzeff, N. B. 2002, ApJ, 579, 671

Watanabe, M. 2006, Master thesis (Waseda Univ.)

Yamasaki, T., & Yamada, S. 2006, to be published in ApJ, astro-ph/0606581

This preprint was prepared with the AAS LaTeX macros v5.2.

Table 1. The mass, radius and Kepler frequency for the proto neutron star model.

$M/M_\odot$	R(km)	Ω_k(Hz)
1.492	55.6	1074

Table 2. Key quantities for *g*-modes in the proto neutron star.

ℓ	Mode	$\bar{\omega}$	ν (Hz)	$E(10^{53}\mathrm{erg})$	a	b
1	g_1^s	2.92	499	5.70	3.50E-03	1.72E-03
	g_2^c	1.43	245	1.30	2.13E-02	−2.99E-04
	g_3^s	1.03	176	1.97	1.67E-03	−1.54E-04
2	g_1^s	3.15	538	7.51	5.91E-03	9.97E-04
	g_2^c	2.24	383	3.15	2.02E-03	−1.01E-04
	g_3^s	1.72	294	7.11	1.02E-03	2.38E-04

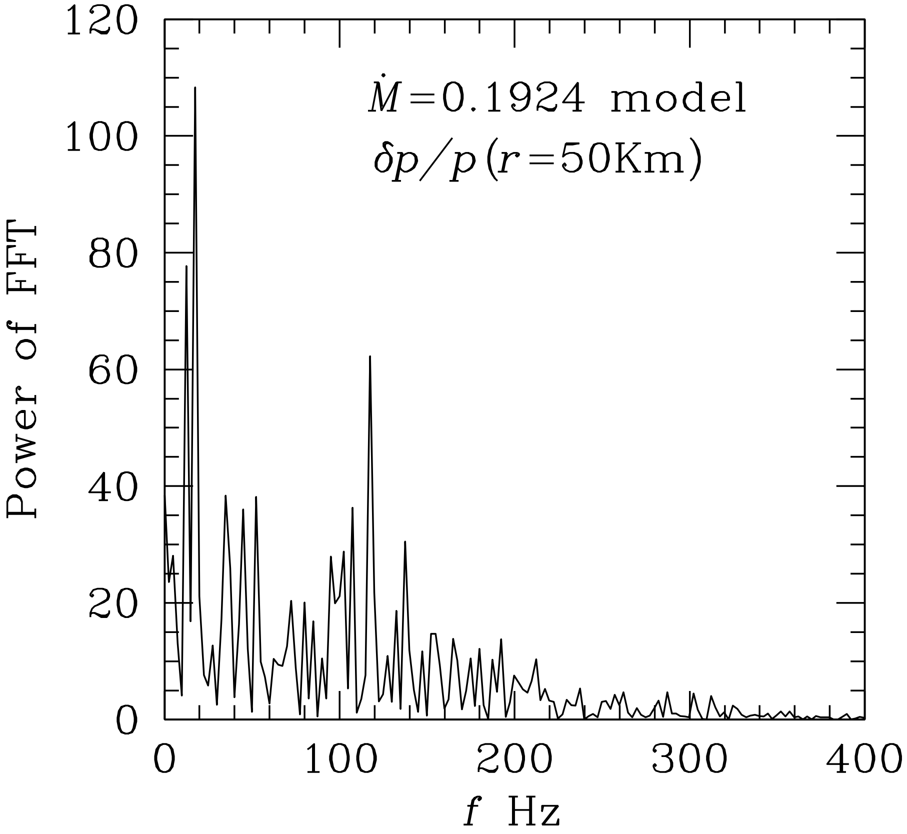

Fig. 1.— Power spectrum of the fractional pressure variation at $r = 50$km, given as a function of the frequency. Here, the fractional pressure variation is expanded in terms of spherical harmonics, and the fractional pressure variation associated with $\ell = 1$ and $m = 0$ is displayed.

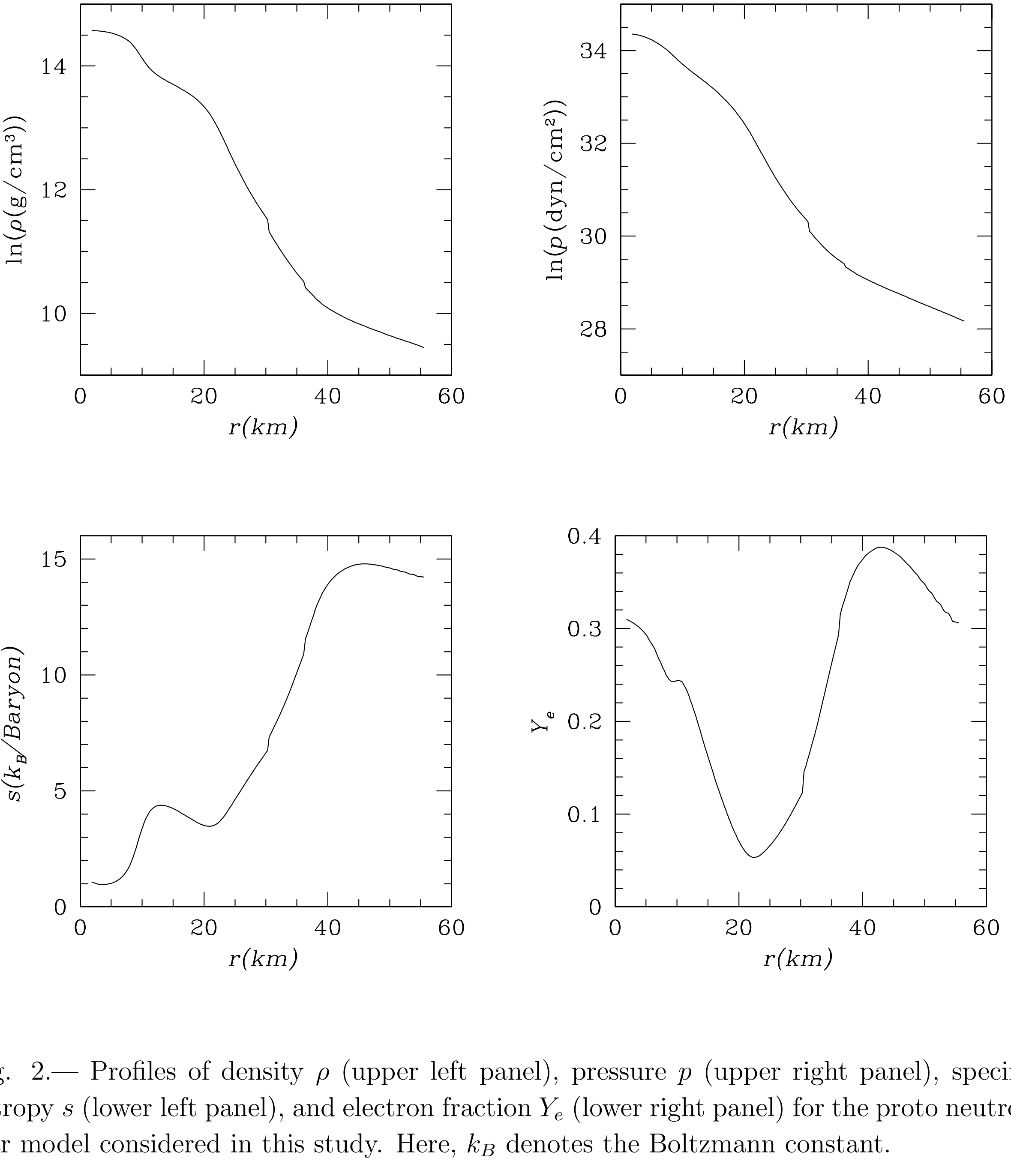

Fig. 2.— Profiles of density ρ (upper left panel), pressure p (upper right panel), specific entropy s (lower left panel), and electron fraction Y_e (lower right panel) for the proto neutron star model considered in this study. Here, k_B denotes the Boltzmann constant.

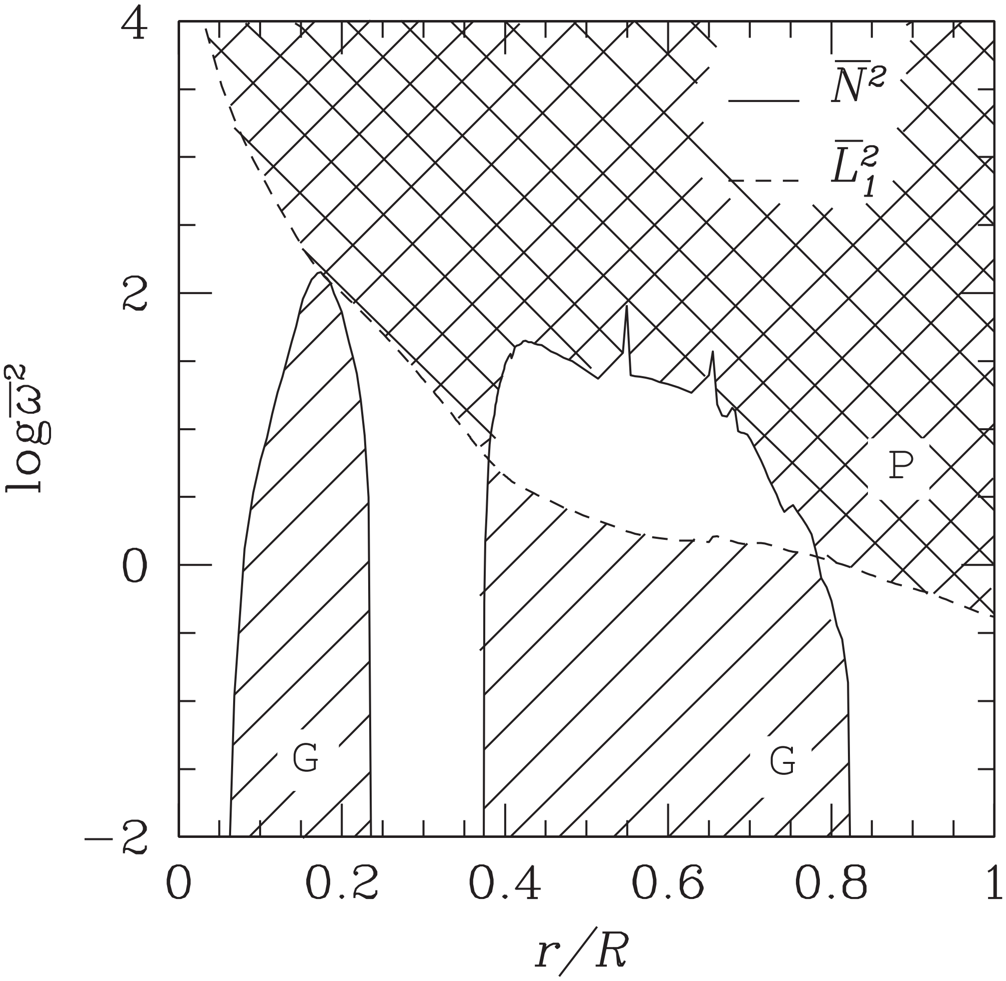

Fig. 3.— Propagation diagram for the proto neutron star model given in Fig. 2, in which the square of the Lamb frequency L_ℓ^2 for $\ell = 1$ and the Brunt-Väisälä frequency N^2 are shown as a function of the normalized radius of the star r/R. The frequency is normalized according to Eq. (15). The *g*- and *p*-mode propagation zones are indicated as the hatched and cross-hatched regions, respectively.

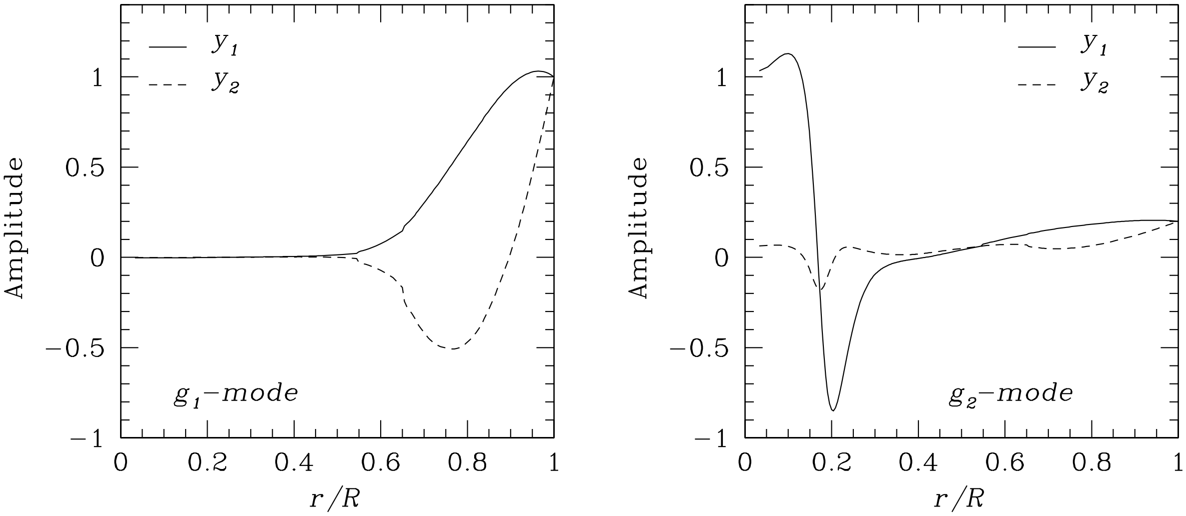

Fig. 4.— Eigen functions y_1 and y_2 as a function of the normalized radius r/R for the g_1-mode (left) and g_2-mode (right) with $\ell = 1$ for the proto neutron star model given in Fig. 2.

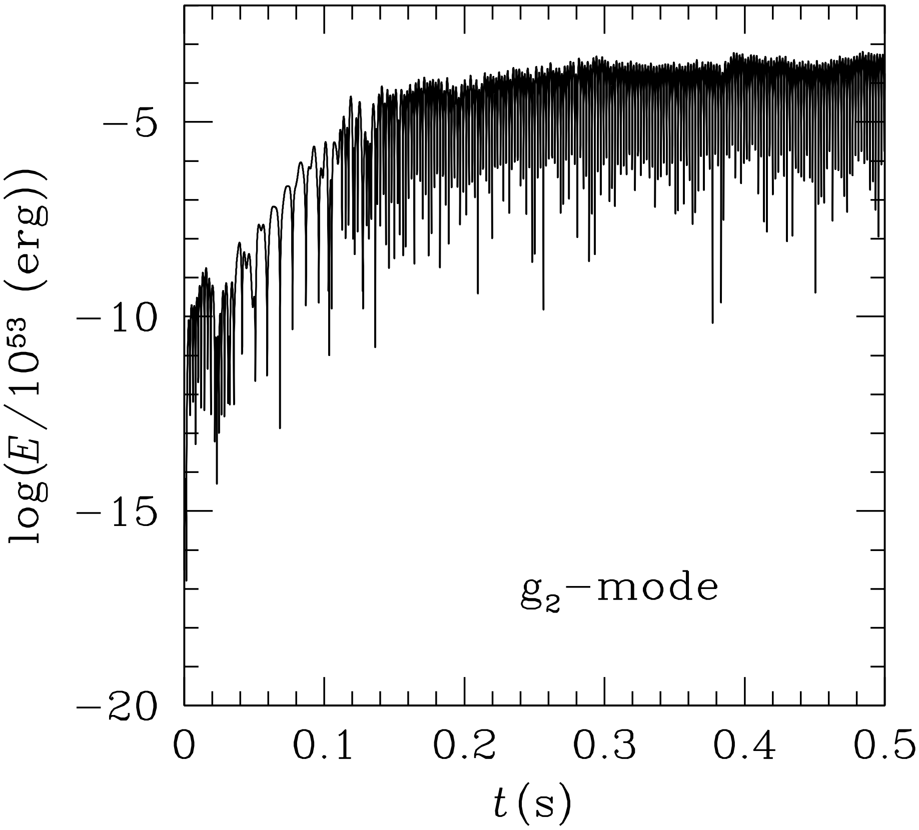

Fig. 5.— Time evolution of the mode energy for the g_2-mode with $\ell = 1$ for the proto neutron star model given in Fig. 2.

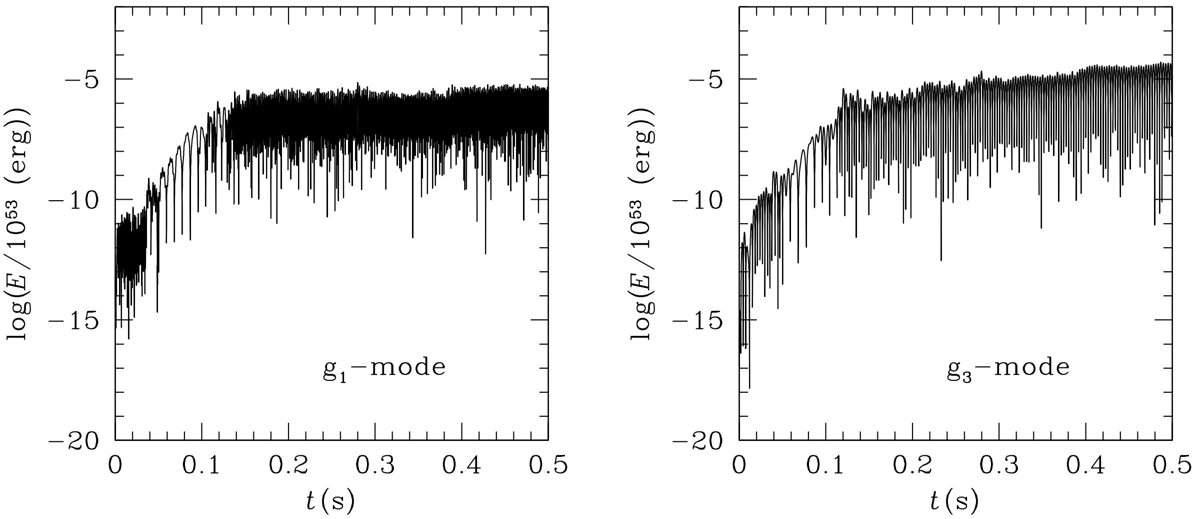

Fig. 6.— Time evolution of the mode energy for the g_1-mode (left) and g_3-mode (right) with $\ell = 1$ for the proto neutron star model given in Fig. 2.